



Alterations of Both Dendrite Morphology and Weaker Electrical Responsiveness in the Cortex of Hip Area Occur Before Rearrangement of the Motor Map in Neonatal White Matter Injury Model

Yoshitomo Ueda¹, Yoshio Bando², Sachiyo Misumi¹, Shino Ogawa^{1,3}, Akimasa Ishida¹, Cha-Gyun Jung¹, Takeshi Shimizu¹ and Hideki Hida^{1*}

OPEN ACCESS

Edited by:

Masahiro Tsuji,
Kyoto Women's University, Japan

Reviewed by:

Jacques-Olivier Coq,
UMR7289 Institut de Neurosciences
de la Timone (INT), France
Lauren Jantzie,
University of New Mexico,
United States

*Correspondence:

Hideki Hida
hhida@med.nagoya-cu.ac.jp

Specialty section:

This article was submitted to
Pediatric Neurology,
a section of the journal
Frontiers in Neurology

Received: 05 January 2018

Accepted: 25 May 2018

Published: 19 June 2018

Citation:

Ueda Y, Bando Y, Misumi S, Ogawa S,
Ishida A, Jung C-G, Shimizu T and
Hida H (2018) Alterations of Both
Dendrite Morphology and Weaker
Electrical Responsiveness in the
Cortex of Hip Area Occur Before
Rearrangement of the Motor Map in
Neonatal White Matter Injury Model.
Front. Neurol. 9:443.
doi: 10.3389/fneur.2018.00443

¹ Department of Neurophysiology and Brain Science, Nagoya City University Graduate School of Medical Sciences, Nagoya, Japan, ² Department of Functional Anatomy and Neuroscience, Asahikawa Medical University, Asahikawa, Japan, ³ Department of Obstetrics and Gynecology, Nagoya City University Graduate School of Medical Sciences, Nagoya, Japan

Hypoxia-ischemia (H-I) in rats at postnatal day 3 causes disorganization of oligodendrocyte development in layers II/III of the sensorimotor cortex without apparent neuronal loss, and shows mild hindlimb dysfunction with imbalanced motor coordination. However, the mechanisms by which mild motor dysfunction is induced without loss of cortical neurons are currently unclear. To reveal the mechanisms underlying mild motor dysfunction in neonatal H-I model, electrical responsiveness and dendrite morphology in the sensorimotor cortex were investigated at 10 weeks of age. Responses to intracortical microstimulation (ICMS) revealed that the cortical motor map was significantly changed in this model. The cortical area related to hip joint movement was reduced, and the area related to trunk movement was increased. Sholl analysis in Golgi staining revealed that layer I-III neurons on the H-I side had more dendrite branches compared with the contralateral side. To investigate whether changes in the motor map and morphology appeared at earlier stages, ICMS and Sholl analysis were also performed at 5 weeks of age. The minimal ICMS current to evoke twitches of the hip area was higher on the H-I side, while the motor map was unchanged. Golgi staining revealed more dendrite branches in layer I-III neurons on the H-I side. These results revealed that alterations of both dendrite morphology and ICMS threshold of the hip area occurred before the rearrangement of the motor map in the neonatal H-I model. They also suggest that altered dendritic morphology and altered ICMS responsiveness may be related to mild motor dysfunction in this model.

Keywords: hypoxia-ischemia in premature infants, white matter injury, intracortical microstimulation (ICMS), golgi staining, cortical layer I-III, hip area, dendritic branches

INTRODUCTION

Although advances of perinatal medicine have improved the survival rate of preterm infants (1, 2), these infants often have neurological insults due to hypoxia-ischemia (H-I) accompanied with brain immaturity (3). A profound shift in the features of H-I over time has also been reported: a milder form of H-I, characterized by nondestructive lesions, is reportedly increasing in prevalence (4–7). However, there is a pressing need to expand current understanding of the mechanisms underlying the effects of brain insult and to develop treatments for the resulting behavioral and cognitive dysfunction in development.

Preterm infants have a higher risk of neonatal white matter injury (WMI) because late oligodendrocyte progenitor cells (OPC), which are abundant at gestational weeks 20–28 in humans (8), are particularly susceptible to H-I (9–11). Ischemia-induced neuroinflammation and prenatal inflammatory response are known to be related to neonatal WMI (12–15). Neonatal WMI causes neurodevelopmental deficits during development, including motor deficits (such as cerebral palsy), learning disorders, and behavioral difficulties (including attention deficit/hyperactivity disorder) (16–18). Various animal models of preterm infants have been reported, including models using sheep (19, 20), rabbit (21–23), piglets (24–26), and rodents (15, 27–32). Among the available rodent models, the Rice-Vannucci model (33) and its variations have been commonly used (27, 28, 30). Other models, created by unilateral uterine artery ligation of dams at embryonic day (E) 17 (34, 35) or transient bilateral occlusion of the uterine arteries at E18 (15, 29, 31), have also been reported.

We previously established a rat model of neonatal WMI produced by right carotid artery occlusion followed by under 6% oxygen for 1 h (36), based on the notion that late development of OPC (preOLs) in the immature brain is specifically associated with vulnerability to H-I (11). In this neonatal WMI model, actively proliferating OL progenitors are primarily damaged, with a decreased number of mature OL cells and hypomyelination in the sensorimotor cortex in adulthood, indicating that impaired motor coordination is induced by impaired myelination in layer I–IV rather than neuronal loss (37). This neonatal WMI model exhibited moderate motor deficits, especially in the hindlimbs, accompanied with disorganization of oligodendrocyte development in layers II–III of the sensorimotor cortex (38).

As neonatal WMI is a complex amalgam of destructive developmental disturbances in premature infants (5), changes in neuronal circuit formation and connectivity in the cerebral cortex may be affected by the close relationship between neuronal development and myelination. Although our model has revealed motor coordination dysfunction without the loss of cortical neurons (37, 38), it remains unclear how motor dysfunction is induced in this model.

To reveal the mechanisms underlying imbalanced motor coordination in the neonatal WMI model, we investigated electrical responsiveness, and dendrite morphology in the sensorimotor cortex in adulthood. Thus, intracortical microstimulation (ICMS) in the hindlimb motor cortex was performed to reveal electrophysiological responses, and

morphological changes were examined in the motor cortex using Golgi staining.

We found that the cortical motor map was significantly changed in neonatal WMI model at 10 weeks of age: the cortical area related to hip joint movement was reduced while the area related to trunk movement was increased. In addition, we found that layer I–III neurons on the H-I side had more dendrite branches compared with the contralateral side in Golgi staining. ICMS and Golgi staining performed at 5 weeks of age revealed that the minimal ICMS current to evoke twitches was higher on the H-I side while the motor map was unchanged, and more dendrite branches in layer I–III neurons were shown in the H-I side, indicating that alterations of both dendrite morphology and ICMS threshold of the hip area occurred before the rearrangement of the motor map in the neonatal H-I model.

MATERIALS AND METHODS

Animals

Animal care was carried out according to the guidelines of the Institute for Experimental Animal Sciences, Nagoya City University Graduate School of Medical Sciences, Nagoya, Japan. All experimental procedures were approved by the committee of animal experimentation of Nagoya City University Medical School, and appropriate measures were taken to minimize the pain and discomfort of the animals used in the study. Until weaning, 10 male Wistar rat pups (Japan SLC, Japan) were reared with a foster mother. After weaning, 3–5 rats were housed together in each cage. A total of 48 rats from multiple different litters were euthanized for this study, including 17 rats as controls, and 31 rats as neonatal H-I models.

Neonatal WMI Model

A procedure involving H-I treatment was conducted to produce neonatal WMI model, as we confirmed many characteristics of the injury in the white matter in our previous papers (36–38). Rat pups at postnatal day 3 (P 3) were subjected to right common carotid artery cauterization under isoflurane (Pfizer, NY, USA) anesthesia (5% [v/v] induction, 1.0% [v/v]) and kept at 37°C on a heat pad. After a 2-h recovery period with their dam, pups were exposed to 6% (v/v) O₂ hypoxia for 60 min in a container submerged in a 38°C water bath.

As a control condition, we performed 6% hypoxia after a sham operation: skin incision, separation around the right common carotid artery and skin suture were performed before the hypoxia. We used this condition as controls for ICMS because we previously confirmed that there was no significant difference between “sham operation with normoxia” and “sham operation with 6% hypoxia” in histology (the numbers of neurons and microglia, the morphology of microglia, and the intensity of myelin basic protein staining) or behavior (motor function by motor deficit score) (38).

Intracerebral Microstimulation (ICMS)

We first performed ICMS at 10 weeks of age to investigate differences in the pattern of motor maps ($n = 9$ for neonatal WMI and $n = 8$ for controls). ICMS was then performed at 5 weeks of

age to reveal the developmental pattern of the change ($n = 11$ for neonatal WMI and $n = 9$ for controls), using a procedure similar to methods described elsewhere (39–41) with some modifications (42).

Rats underwent anesthesia with a mixture of ketamine (60 mg/kg, i.p.) and xylazine (10 mg/kg, i.p.), and dexamethasone (0.1 mg/kg) was then administered into the right gluteal fascia to prevent brain edema. Thirty minutes after the first injection, a mixture of ketamine (30 mg/kg) and xylazine (5 mg/kg) was injected into the right gluteal fascia to maintain constant anesthesia during cranial scraping. Supplemental injection of ketamine (40 mg/kg), or a mixture of ketamine (15 mg/kg) and xylazine (2.5 mg/kg), was occasionally used when animals exhibited vibrissae twitching, muscle twitching and/or tachypnea during recording, followed by a 10-min break from recording to keep the measurement consistent.

Rats were fixed on a stereotaxic apparatus (Narishige, Japan), and craniotomy was performed to expose the right sensorimotor cortex. The coordinates for the openings were 1.0–3.0 mm posterior and 1.0–3.0 mm lateral from the bregma, known as the sensorimotor area, including the hindlimb area. The exposed area was regularly spaced out over a 0.5-mm grid. Under a microscope, a glass-insulated tapered tungsten electrode (250 μm shank diameter, impedance, 0.7 M Ω ; Alpha Omega #380-080607-11, GA, USA) was lowered perpendicularly into the cortex to 1,600 μm below the cortical surface, a depth corresponding to layer V of the sensorimotor cortex. The electrode was then adjusted by $\pm 200 \mu\text{m}$ to find the appropriate location for measuring the spike pattern with an oscilloscope and loudspeaker. Thirty biphasic pulses (333 Hz, 200 μs pulse duration) produced by an electrical stimulator (Nihon Kohden, Japan) connected to an isolator (Nihon Kohden, Japan) were passed through the electrode every 2 s, and the response of the cortex was amplified using an amplifier (AM Systems, WA, the USA) connected to an oscilloscope. Starting at a current of 0 μA , intensity was increased in 10 μA steps until twitching of the hip joint, knee joint, foot joint, digit and trunk were confirmed by palpation and/or visual inspection. The current was then gradually decreased until the twitch was no longer detectable. This level was defined as the current threshold. If no twitches were evoked at 200 μA , the site was defined as “non-responsive.”

ICMS data are represented as cortical maps with current thresholds in **Figure 1**, (**Supplemental Figure 1**, and as heat maps in **Figures 2A, 4A**. Cortical maps were created using areas that responded to the stimulation and are shown as 5-colored code in the grid: in each animal, we noted for each stimulated square whether the stimulation resulted in twitching of the hip joint (red), knee joint (yellow), foot joint (light blue), and trunk (green), or the non-responsive square (gray). The generated heat maps represent the occurrence rate of each stimulated spot in the sensorimotor area, and were calculated separately for each experimental group: for each point, the number of animals in which the movement was elicited was taken over the number of times that spot was stimulated in each group. For example, if three animals in a group responded to cortical stimulation at a cortical spot when five of the animals in the group were stimulated at that point, the occurrence rate would be 0.6.

To visualize the organization of the cortical spots with higher occurrence rates of the movements, a 4-grade white-black code was applied to the map.

Golgi Staining

We used an FD Rapid GolgiStain Kit (COSMO BIO, Japan) for Golgi staining according to the standard protocol (43). The rats were deeply anesthetized with sodium pentobarbital, and cervical dislocation was performed. Coronal brain sections of 2 mm thickness (1.0–3.0 mm posterior to the bregma, which was the same area used for ICMS) were obtained using a brain matrix and soaked in Golgi-Cox solution for 14 days followed by 30% sucrose for 3 days. The sections were sliced into 200 μm , stained and photographed with BZ-X700 (Keyence, Japan) focusing on the motor cortex (same area for ICMS), particularly layers I–III.

Based on our previous paper (44), we used Sholl analysis to evaluate dendrite expansion from a cell body: the numbers of cross sections at every 20- μm from center of the cell body were counted in 27 Golgi-positive neurons per animal (neonatal WMI model: $n = 4$ at 5 weeks of age and $n = 5$ at 10 weeks of age; sham-operated control: $n = 1$).

Immunohistochemistry for Microglia

We performed immunohistochemistry at P 17 ($n = 4$) and P 28 ($n = 4$). Under deep anesthesia with pentobarbital (>50 mg/kg), rats were perfused with 4% paraformaldehyde in 0.1 M phosphate buffered saline (PBS). The brains were obtained, post-fixed with the same fixative overnight, and cryoprotected with 30% sucrose. Coronal-sections (40 μm) were prepared from 1–3 mm posterior to the bregma that contains the sensorimotor cortex of the hindlimb area. After soaking with 0.25% Triton X-100 in PBS (PBS-T), blocking was performed with 10% normal goat serum (NGS) (Vector Labs, USA) for 60 min. The slices were reacted with anti-Iba1 polyclonal antibody (1:1,000; Wako, Japan) immersed in PBS-T containing 1% NGS at 4°C overnight, followed by immersion goat anti-rabbit IgG conjugated with Alexa Fluor 594 (1:1,000; Abcam, UK). After the slices were embedded on a glass slide with mounting medium (Vector Labs, USA), slices were photographed with a fluorescence microscope (Axio Observer.Z1; Zeiss, Germany) and an AX70 microscope (Olympus, Japan).

Statistics

Mann–Whitney U -tests were used to compare the current threshold and the number of blocks between control and neonatal WMI rats in the ICMS experiment. Mann–Whitney U -tests were also used to compare the number of cross sections between ipsilateral side and contralateral side in Sholl analysis. All data are shown as mean \pm standard error of the mean (SEM).

RESULTS

Motor Map Change of the Neonatal WMI Model in Adulthood at 10 Weeks of Age

To examine neuronal responsiveness in the sensorimotor cortex, we performed ICMS focusing on the right H-I side compared with the right control side at 10 weeks of age (**Figures 1, 2**). We

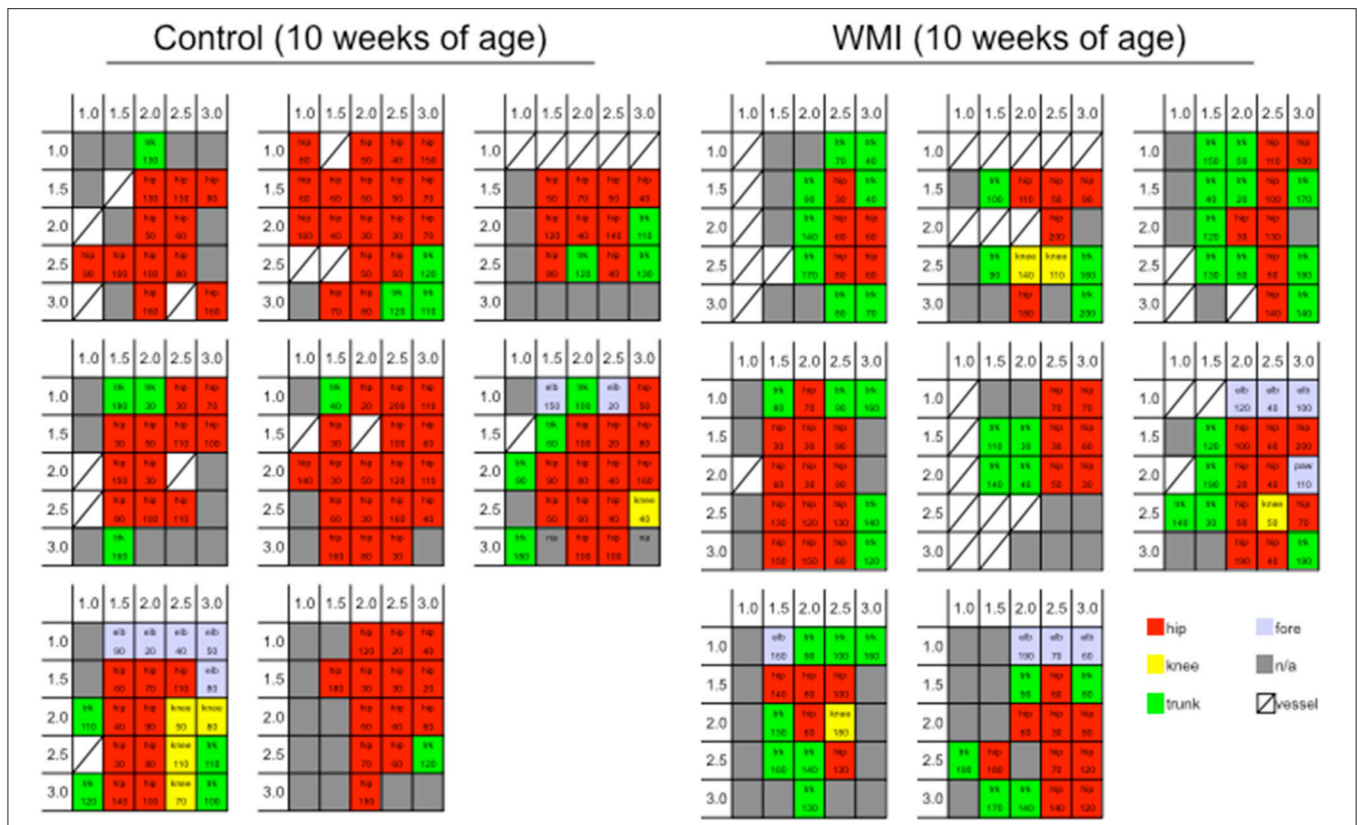


FIGURE 1 | Cortical motor map by ICMS at 10 weeks of age. We stimulated the sensorimotor cortex per 0.5 mm at 1.0–3.0 mm right and 1.0–3.0 mm posterior from the bregma. Each grid shows a cortical map of each rat cortex in control group ($n = 8$) and neonatal WMI group ($n = 8$). Blocks in the grids show the portion of the rat body in which twitching was observed (hip joint, knee joint, trunk, and forelimb), and the current threshold is presented in each grid. Cortical maps are shown as a 5-colored code in the grid: twitching of the hip joint (red), knee joint (yellow), foot joint (light blue), and trunk (green), and non-responsive square (gray).

stimulated the hindlimb area of the sensorimotor cortex because gross hindlimb function exhibited more disruption than forelimb function in our previous study (37, 38).

Each cortical map in the control group ($n = 8$) and neonatal WMI group ($n = 8$) is shown in **Figure 1**. To clarify the map expansion of each group, we re-organized the map data into heat maps of the hip and the trunk (**Figure 2A**). The heat maps clearly revealed a decrease in the size of the hip area and enlargement of the trunk area in the WMI group. The number of blocks in the hip area and the trunk area confirmed a significant decrease in the hip area (control: 12.8 ± 1.3 , $n = 8$; WMI: 7.5 ± 1.0 , $n = 8$; $p < 0.01$) and a significant increase in the trunk area (control: 2.5 ± 0.5 , $n = 8$; WMI: 5.9 ± 0.8 , $n = 8$; $p < 0.01$) (**Figure 2B**). In contrast, the current threshold for evoking the movements remained unchanged in both the hip joint (control: $78.2 \pm 4.3 \mu\text{A}$; WMI: $87.6 \pm 6.2 \mu\text{A}$) and trunk muscle (control: $112 \pm 8.57 \mu\text{A}$; WMI: $114 \pm 7.26 \mu\text{A}$) (**Figure 2C**).

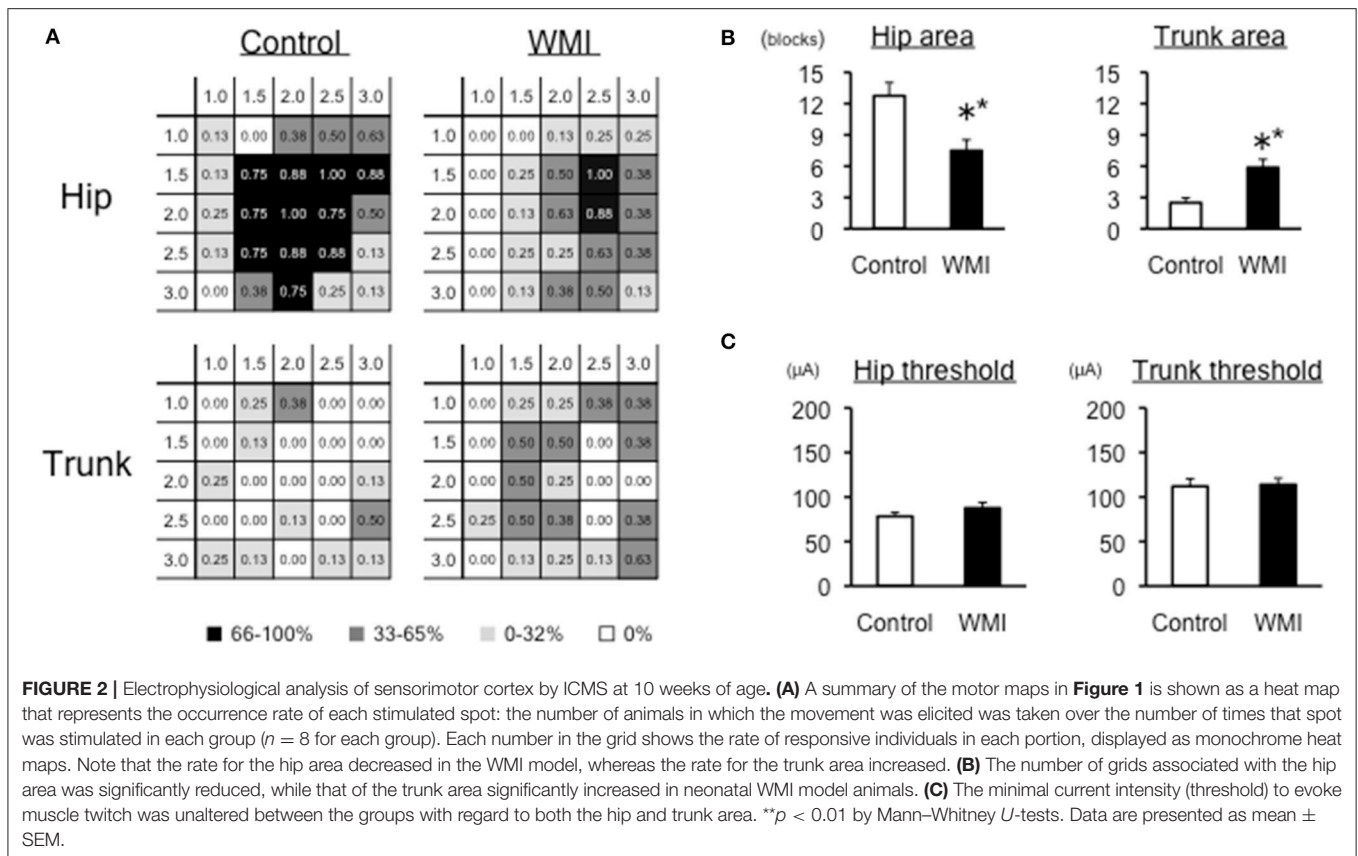
Change of Dendrite Expansion in the Neonatal WMI Model in Adulthood

To investigate whether neuronal morphology changed at 10 weeks of age, when cortical map reorganization was altered, we performed Golgi staining focusing on the same sensorimotor

cortex in neonatal WMI rats ($n = 5$) (**Figure 3**). To evaluate developmental changes in morphology, we used Sholl analysis and counted the number of cross sections every 20- μm from the center of the cell body (**Figure 3B**). Neurons in the right H-I hemisphere (ipsilateral side) appeared to exhibit denser expansion of dendrites in layers I–III (**Figure 3A**). A similar pattern of dendrite expansion was observed in layer V of the neonatal WMI model (data not shown), although accurate analysis was difficult due to the higher neuron density. Sholl analysis revealed that neurons on the H-I side had significantly more dendritic branches (**Figure 3B**; **Supplemental Table 1**). In contrast, sham-operated animals exhibited no differences between hemispheres (**Figure 3C**), showing an equivalent number to the contralateral side of the neonatal WMI model (data for the contralateral side in **Figure 3B**).

Electrophysiological and Morphological Changes in Earlier Developmental Stages at 5 Weeks of Age

To determine whether the electrophysiological and morphological changes described above were exhibited at earlier developmental stages, we also performed ICMS and Golgi staining at 5 weeks of age.



At 5 weeks of age, the map size appeared to be smaller than that at 10 weeks old (**Supplemental Figure 1**). The heat map indicated that the size of the hip area of the neonatal WMI group ($n = 11$) was unchanged compared with the control animals ($n = 9$) (**Figure 4A**). The number of blocks in the hip area in each animal was also unaltered between groups (control: 8.1 ± 1.4 ; WMI: 7.5 ± 0.6) (**Figure 4B**). In contrast, the threshold of the hip area was significantly higher in the neonatal WMI group (control, $107 \pm 6.44 \mu\text{A}$; WMI, $127 \pm 5.50 \mu\text{A}$; $p < 0.05$) (**Figure 4C**, **Supplemental Figure 1**). Sholl analysis of layers I–III in the motor area ($n = 4$) indicated that neurons in the right hemisphere had significantly more dendritic branches (**Figure 4D**, **Supplemental Table 1**).

It has been previously reported that microglia have a phagocytotic effect on the elimination of synapses during development (pruning) (45–48). To test the possibility that microglial activation was related to changes in cortical map reorganization (ICMS), Iba1 immunohistochemistry was performed at P 17 and P 28 (before 5 weeks old) because morphological changes of the dendrites (Golgi staining) were already observed at 5 weeks of age.

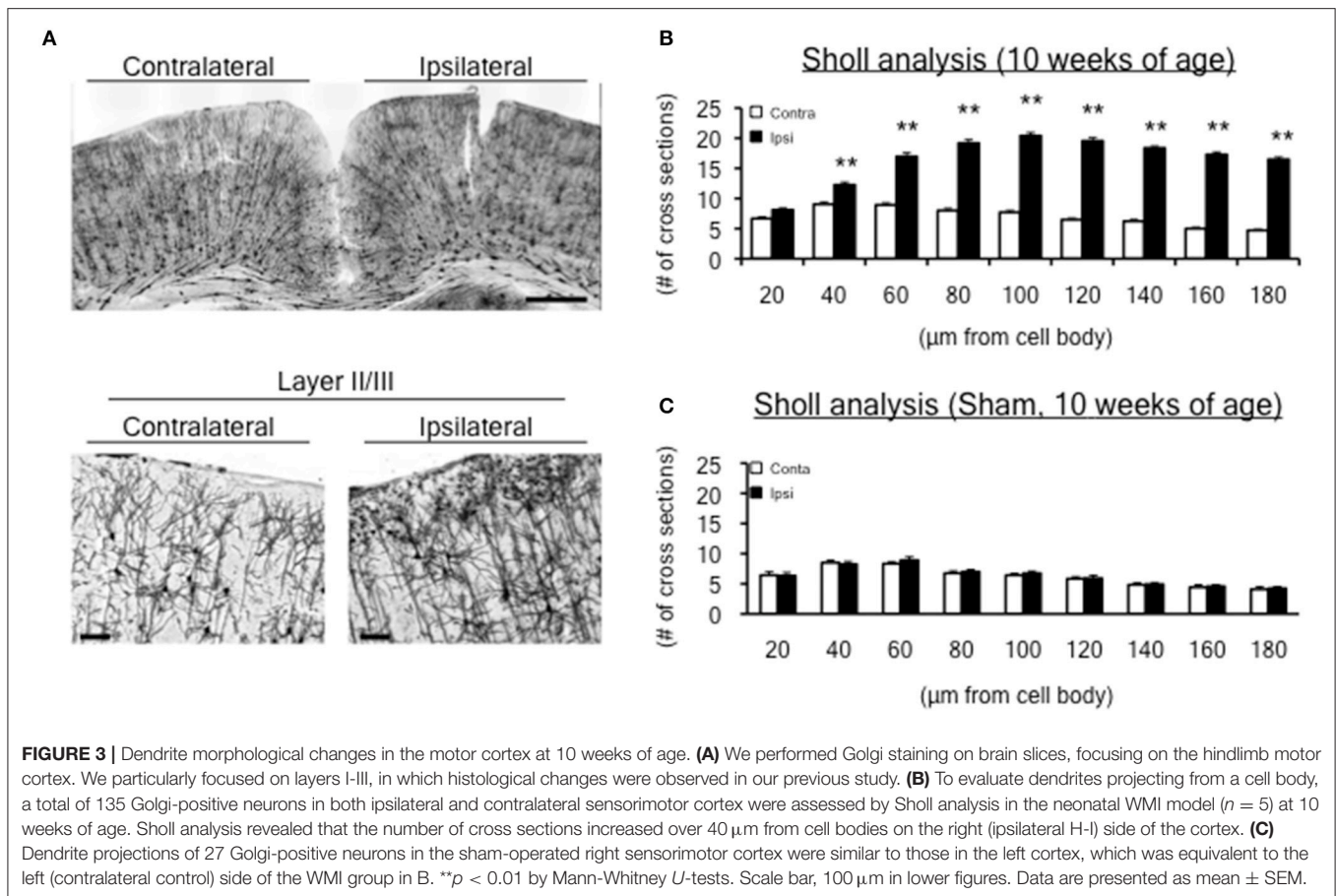
Iba-1 positive cells were detected in the parietal cortex of the neonatal WMI brain (**Supplemental Figure 2A**). There were many Iba-1 positive microglia with amoeboid bodies and thick processes on the H-I side at P 17 ($n = 4$) (**Supplemental Figure 2B**). However, Iba-1 positive cells were not detected in the neonatal WMI model at P 28 ($n = 4$) (**Supplemental Figure 2C**).

DISCUSSION

To elucidate how motor dysfunction in neonatal WMI is induced without the loss of cortical neurons, we investigated electrical responsiveness and dendrite morphology in the sensorimotor cortex in adulthood (10 weeks of age), as well as earlier developmental stages (5 weeks of age) in WMI model. The results revealed that the motor map in the sensorimotor cortex was altered at 10 weeks of age but not 5 weeks of age. However, the threshold of the hip area was higher on the H-I side at 5 weeks of age, while it was similar at 10 weeks of age. In addition, an increased number of dendritic branches in layers I–III were shown in the H-I cortex as early as 5 weeks old, and this increase was maintained until 10 weeks old. Interestingly, activated microglia were detected on the H-I side at P 17, but not at P 28.

Alteration of Motor Maps in the Neonatal WMI Model

It is known that the cortical motor map changes after brain insults such as intracerebral hemorrhage and spinal cord injury, but can be recuperated by rehabilitation (42) and motor training (40). Environmental enrichment is one method for improving behavioral performance, and has been found to promote cortical development (49). Thus, the motor map is closely related to motor function. These previous findings suggest that the alteration of the motor map at 10 weeks of age found in the present study (hip area reduction and trunk area expansion) may



be related to the imbalanced motor coordination in the neonatal WMI model (38). However, alterations of the motor map cannot completely explain the motor imbalance in this model, because it was unchanged at 5 weeks of age in the present study.

A previous study reported that the motor map emerges after 4 weeks old and eventually expands, while gradual decreases of the current threshold are promoted by enriched environments in development (49). These findings indicate that the period after weaning is a critical window in the development of normal function acquisition. Therefore, the higher threshold we detected in the hip area of the WMI group at 5 weeks of age might indicate a developmental delay of functional acquisition, as the threshold became almost equivalent at 10 weeks of age.

Alteration of Dendrite Morphology in the Surface Area of the Cortex

Although both excitatory and inhibitory neurons were maintained in the sensorimotor cortex of this model (37), the surface area was affected, exhibiting oligodendrocyte loss and hypomyelination (37, 38). However, it remains unclear how motor dysfunction is induced in this model. Changes in neuronal circuit formation and connectivity in the cerebral cortex could be induced, as neonatal WMI is a complex amalgam of destructive developmental disturbances in premature infants (5). Morphological changes of dendrites in layers II-III were

also confirmed by detailed analysis with Golgi staining as early as P 28 in the present study. As the surface area in the sensorimotor cortex receives many afferent fibers, the altered dendritic morphology of Golgi-positive neurons in layers II-III, as revealed by Sholl analysis in this study, might change local neuronal circuits and connectivity, causing the motor imbalance observed in this model.

The current study was unable to provide a clear answer regarding the question of how this morphological change in layers II-III is related to the response to ICMS in this model. GABAergic neurons in the sensorimotor cortex should be taken into consideration, as inhibitory neurons are important for normal motor map function (49), and the motor map changes immediately with injection of a GABA receptor antagonist to the motor cortex (50). Although further studies will be required to understand the contribution of GABAergic neurons, it is important to consider the migration mechanisms and temporal excitatory effects of immature GABAergic neurons by P 14-16.

The retardation of OL differentiation (37, 38) is likely to affect cortical development, as OL-expressing proteins such as myelin associated glycoprotein, Nogo-A, and oligodendrocyte-myelin glycoprotein changed neurite outgrowth during development after neonatal hypoxia (51). Thus, changes of dendrite morphology in layers II-III of sensorimotor cortex

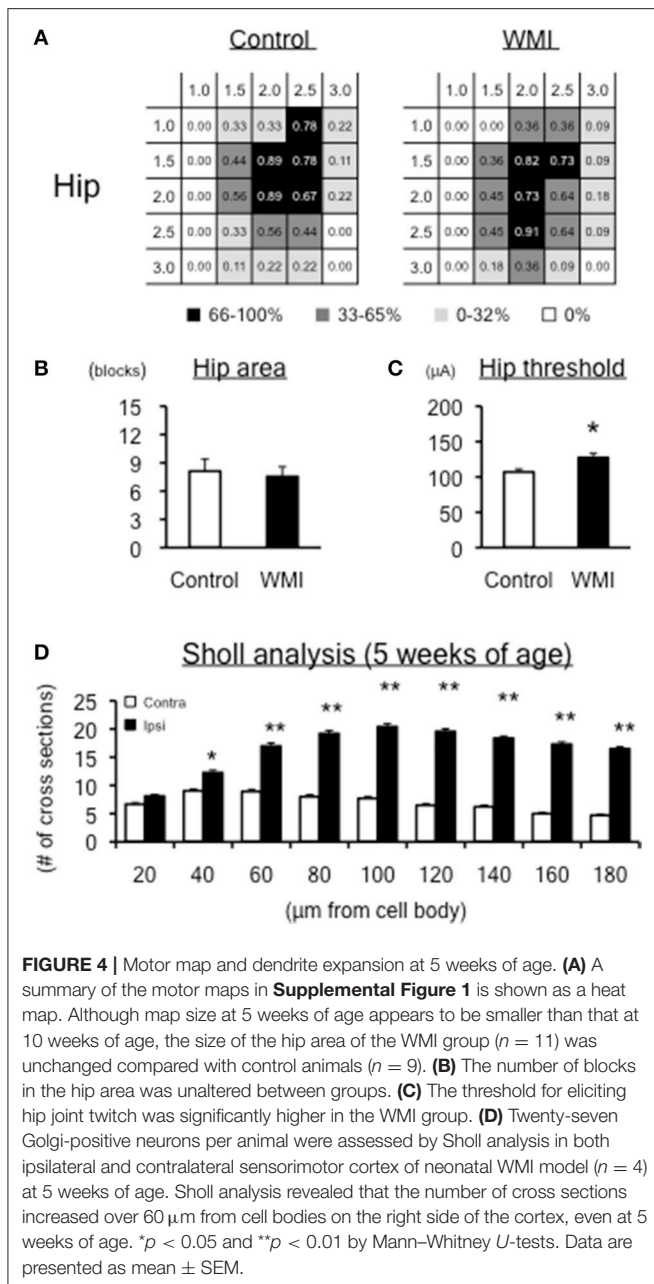


FIGURE 4 | Motor map and dendrite expansion at 5 weeks of age. **(A)** A summary of the motor maps in **Supplemental Figure 1** is shown as a heat map. Although map size at 5 weeks of age appears to be smaller than that at 10 weeks of age, the size of the hip area of the WMI group ($n = 11$) was unchanged compared with control animals ($n = 9$). **(B)** The number of blocks in the hip area was unaltered between groups. **(C)** The threshold for eliciting hip joint twitch was significantly higher in the WMI group. **(D)** Twenty-seven Golgi-positive neurons per animal were assessed by Sholl analysis in both ipsilateral and contralateral sensorimotor cortex of neonatal WMI model ($n = 4$) at 5 weeks of age. Sholl analysis revealed that the number of cross sections increased over 60 μm from cell bodies on the right side of the cortex, even at 5 weeks of age. * $p < 0.05$ and ** $p < 0.01$ by Mann–Whitney U -tests. Data are presented as mean \pm SEM.

in adulthood could be altered by oligodendrocyte loss and hypomyelination (37, 38).

Possible Effects of Iba-1 Positive Microglia

Strong expression of ED1-positive microglial/macrophage cells was detected in the cortex of the model at P 5 in our previous report (36). In this study, the appearance of Iba-1 positive microglia was confirmed in the sensorimotor cortex until P 17, but the cells were unremarkable on both sides of the cortex at P 28.

Previous studies have reported that microglia affect synaptic pruning during development (45–48), and that synapse

maintenance and the stripping function of microglia are related to dendrite expansion (52–54). Thus, it is likely that transient appearance of microglial cells until P 28 affected dendritic changes in the cortex that were detected at 5 weeks of age in this study. Further studies will be necessary to examine the morphology during earlier periods of development, and to elucidate the relationship between microglia and dendrite expansion in more detail.

Limitations of the Study

It should be noted that only male pups were used in this study, as there are several reports about the sex-dependent differences of the response to H-I (55–58). Several points in the present study would be strengthened by further experiments as follows. As our discussion related to possible effects of Iba-1 positive microglia is highly speculative, co-staining of Iba-1 with different antigens or synaptic markers, detection of genes related to pro-inflammatory cytokines, and unbiased quantification of Iba-1 positive microglial number (59, 60) should be performed in future. In addition, small sample size of Golgi-staining of sham-operated animal and lack of true control (sham-operation with normoxia) will be solved in near future. As for the limitations in ICMS experiment, the exact motor map boundaries of the hip and trunk are not outlined in this study due to our large regularly space over a 0.5-mm grid and small sample size of our study. It might be possible to get the exact motor map boundaries using more precise ICMS experiment (35).

CONCLUSION

The current results demonstrated that the neonatal WMI model exhibited alterations of neuronal morphology and cortical responsiveness. Our data also indicated that alterations of dendrite morphology and electrical responses in the cortex occurred before the rearrangement of the motor map in the neonatal WMI model.

AUTHOR CONTRIBUTIONS

ICMS was performed by YU with assistance of AI and Golgi staining was performed by YB with hard assessment by YU and SM. The hypoxia-ischemia model was made by SM with the help by SO, followed Iba1 staining by TS. C-GJ and TS are involved in helpful discussion and joined in writing paper. The draft of this paper was written by YU. HH organizes this study and wrote this paper as correspondence. This study is mainly supported by the grants to SM, YU, and HH with partial support of the grants to C-GJ and TS.

FUNDING

This study was supported by Grants-in-Aid for Scientific Research in priority area (C) (# 26430020 to HH, #16K10100 to SM), and young area (B) (#26860851 to SM, #17K16303 to YU), and a Grant-in-Aid for Research Activity Start-up (#15H06538 to YU) from the Japan Society for the Promotion of Science (JSPS).

This study was also supported by a Grant-in-Aid for Scientific Research on Innovative Areas (Adaptive Circuit Shift) to H.H.

ACKNOWLEDGMENTS

We thank Edanz Group Ltd. for editing a draft of this manuscript.

SUPPLEMENTARY MATERIAL

The Supplementary Material for this article can be found online at: <https://www.frontiersin.org/articles/10.3389/fneur.2018.00443/full#supplementary-material>

REFERENCES

- Saigal S, Doyle LW. An overview of mortality and sequelae of preterm birth from infancy to adulthood. *Lancet* (2008) 371:261–9. doi: 10.1016/S0140-6736(08)60136-1
- Costeloe KL, Hennessy EM, Haider S, Stacey F, Marlow N, Draper ES. Short term outcomes after extreme preterm birth in England: comparison of two birth cohorts in 1995 and 2006 (the EPICure studies). *BMJ* (2012) 345:e7976. doi: 10.1136/bmj.e7976
- Rees S, Inder T. Fetal and neonatal origins of altered brain development. *Early Hum Dev.* (2005) 81:753–61. doi: 10.1016/j.earlhumdev.2005.07.004
- Inder TE, Anderson NJ, Spencer C, Wells S, Volpe JJ. White matter injury in the premature infant: a comparison between serial cranial sonographic and MR findings at term. *Am J Neuroradiol.* (2003) 24:805–09.
- Volpe JJ. Brain injury in premature infants: a complex amalgam of destructive and developmental disturbances. *Lancet Neurol.* (2009) 8:110–24. doi: 10.1016/S1474-4422(08)70294-1
- Back SA, Rosenberg PA. Pathophysiology of glia in perinatal white matter injury. *Glia* (2014) 62:1790–815. doi: 10.1002/glia.22658
- Tutor N, Benders MJ, Counsell SJ, Nongena P, Ederies MA, Falconer S, et al. Punctate white matter lesions associated with altered brain development and adverse motor outcome in preterm infants. *Sci Rep.* (2017) 7:13250. doi: 10.1038/s41598-017-13753-x
- Craig A, Ling Luo N, Beardsley DJ, Wingate-Pearse N, Walker DW, Hohimer AR, et al. Quantitative analysis of perinatal rodent oligodendrocyte lineage progression and its correlation with human. *Exp Neurol* (2003) 181:231–40. doi: 10.1016/S0014-4886(03)00032-3
- Back SA, Gan X, Li Y, Rosenberg PA, Volpe JJ. Maturation-dependent vulnerability of oligodendrocytes to oxidative stress-induced death caused by glutathione depletion. *J Neurosci.* (1998) 18:6241–53. doi: 10.1523/JNEUROSCI.18-16-06241.1998
- Back SA, Luo NL, Borenstein NS, Levine JM, Volpe JJ, Kinney HC. Late oligodendrocyte progenitors coincide with the developmental window of vulnerability for human perinatal white matter injury. *J Neurosci.* (2001) 21:1302–12. doi: 10.1523/JNEUROSCI.21-04-01302.2001
- Back SA, Han BH, Luo NL, Chricton CA, Xanthoudakis S, Tam J, et al. Selective vulnerability of late oligodendrocyte progenitors to hypoxia-ischemia. *J Neurosci.* (2002) 22:455–63. doi: 10.1523/JNEUROSCI.22-02-00455.2002
- Saadani-Makki F, Kannan S, Lu X, Janisse J, Dawe E, Edwin S, et al. Intrauterine administration of endotoxin leads to motor deficits in a rabbit model: a link between prenatal infection and cerebral palsy. *Am J Obstet Gynecol.* (2008) 199:651.e1-7. doi: 10.1016/j.ajog.2008.06.090
- Wang X, Stridh L, Li W, Dean J, Elmgren A, Gan L, et al. Lipopolysaccharide sensitizes neonatal hypoxic-ischemic brain injury in a MyD88-dependent manner. *J Immunol.* (2009) 183:7471–77. doi: 10.4049/jimmunol.090762
- Falahati S, Breu M, Waickman AT, Phillips AW, Arauz EJ, Snyder S, et al. Ischemia-induced neuroinflammation is associated with disrupted development of oligodendrocyte progenitors in a model of periventricular leukomalacia. *Dev Neurosci.* (2013) 35:182–96. doi: 10.1159/000346682
- Jantzie LL, Corbett CJ, Berglass J, Firl DJ, Flores J, Mannix R, et al. Complex pattern of interaction between in utero hypoxia-ischemia and intra-amniotic inflammation disrupts brain development and motor function. *J Neuroinflammation* (2014) 11:131. doi: 10.1186/1742-2094-11-131
- Skranes J, Vangberg TR, Kulseng S, Indredevik MS, Evensen KA, Martinussen M, et al. Clinical findings and white matter abnormalities seen on diffusion tensor imaging in adolescents with very low birth weight. *Brain* (2007) 130:654–66. doi: 10.1093/brain/awm001
- Bora S, Pritchard VE, Chen Z, Inder TE, Woodward LJ. Neonatal cerebral morphometry and later risk of persistent inattention/hyperactivity in children born very preterm. *J Child Psychol Psychiatry* (2014) 55:828–38. doi: 10.1111/jcpp.12200
- van Tilborg E, Heijnen CJ, Benders MJ, van Bel F, Fleiss B, Gressens P, et al. Impaired oligodendrocyte maturation in preterm infants: potential therapeutic targets. *Prog Neurobiol.* (2016) 136:28–49. doi: 10.1016/j.pneurobio.2015.11.002
- Baburamani AA, Castillo-Melendez M, Walker DW. VEGF expression and microvascular responses to severe transient hypoxia in the fetal sheep brain. *Pediatr Res.* (2013) 73:310–6. doi: 10.1038/pr.2012.191
- Drury PP, Davidson JO, Bennet L, Booth LC, Tan S, Fraser M, et al. Partial neural protection with prophylactic low-dose melatonin after asphyxia in preterm fetal sheep. *J Cereb Blood Flow Metab.* (2014) 34:126–35. doi: 10.1038/jcbfm.2013.174
- Derrick M, Luo NL, Bregman JC, Jilling T, Ji X, Fisher K, et al. Preterm fetal hypoxia-ischemia causes hypertonia and motor deficits in the neonatal rabbit: a model for human cerebral palsy? *J Neurosci.* (2004) 24:24–34. doi: 10.1523/JNEUROSCI.2816-03.2004
- Derrick M, Drobyshvsky A, Ji X, Tan S. A model of cerebral palsy from fetal hypoxia-ischemia. *Stroke* (2007) 38:731–5. doi: 10.1161/01.STR.0000251445.94697.64
- Buser JR, Segovia KN, Dean JM, Nelson K, Beardsley D, Gong X, et al. Timing of appearance of late oligodendrocyte progenitors coincides with enhanced susceptibility of preterm rabbit cerebral white matter to hypoxia-ischemia. *J Cereb Blood Flow Metab.* (2010) 30:1053–65. doi: 10.1038/jcbfm.2009.286
- Greenwood K, Cox P, Mehmet H, Penrice J, Amess PN, Cady EB, et al. Magnesium sulfate treatment after transient hypoxia-ischemia in the newborn piglet does not protect against cerebral damage. *Pediatr Res.* (2000) 48:346–50. doi: 10.1203/00006450-200009000-00014
- Robertson NJ, Faulkner S, Fleiss B, Bainbridge A, Andorka C, Price D, et al. Melatonin augments hypothermic neuroprotection in a perinatal asphyxia model. *Brain* (2013) 136:90–105. doi: 10.1093/brain/awt285
- Robertson NJ, Kato T, Bainbridge A, Chandrasekaran M, Iwata O, Kapetanakis A, et al. Methyl-isobutyl amiloride reduces brain Lac/NAA, cell death and microglial activation in a perinatal asphyxia model. *J Neurochem.* (2013) 124:645–57. doi: 10.1111/jnc.12097
- Sizonenko SV, Sirimanne E, Mayall Y, Gluckman PD, Inder T, Williams C. Selective cortical alteration after hypoxic-ischemic

- injury in the very immature rat brain. *Pediatr Res.* (2003) 54:263–9. doi: 10.1203/01.PDR.0000072517.01207.87
28. Fan LW, Lin S, Pang Y, Lei M, Zhang F, Rhodes PG, et al. Hypoxia-ischemia induced neurological dysfunction and brain injury in the neonatal rat. *Behav Brain Res.* (2005) 165:80–90. doi: 10.1016/j.bbr.2005.06.033
 29. Robinson S, Petelenz K, Li Q, Cohen ML, Dechant A, Tabrizi N, et al. Developmental changes induced by graded prenatal systemic hypoxic-ischemic insults in rats. *Neurobiol Dis.* (2005) 18:568–81. doi: 10.1016/j.nbd.2004.10.024
 30. Sizonenko SV, Kiss JZ, Inder T, Gluckman PD, Williams CE. Distinctive neuropathologic alterations in the deep layers of the parietal cortex after moderate ischemic-hypoxic injury in the P3 immature rat brain. *Pediatr Res.* (2005) 57:865–72. doi: 10.1203/01.PDR.0000157673.36848.67
 31. Mazur M, Miller RH, Robinson S. Postnatal erythropoietin treatment mitigates neural cell loss after systemic prenatal hypoxic-ischemic injury. *J Neurosurg Pediatr.* (2010) 6:206–21. doi: 10.3171/2010.5.PEDS.1032
 32. Tsuji M, Ohshima M, Taguchi A, Kasahara Y, Ikeda T, Matsuyama T. A novel reproducible model of neonatal stroke in mice: comparison with a hypoxia-ischemia model. *Exp Neurol.* (2013) 247:218–25. doi: 10.1016/j.expneurol.2013.04.015
 33. Rice JE III, Vannucci RC, Brierley JB. The influence of immaturity on hypoxic-ischemic brain damage in the rat. *Ann Neurol.* (1981) 9:131–41. doi: 10.1002/ana.410090206
 34. Delcour M, Russier M, Xin DL, Massicotte VS, Barbe MF, Coq JO. Mild musculoskeletal and locomotor alterations in adult rats with white matter injury following prenatal ischemia. *Int J Dev Neurosci.* (2011) 29:593–607. doi: 10.1016/j.ijdevneu.2011.02.010
 35. Delcour M, Olivier P, Chambon C, Pansiot J, Russier M, Liberge M, et al. Neuroanatomical, sensorimotor and cognitive deficits in adult rats with white matter injury following prenatal ischemia. *Brain Pathol.* (2012) 22:1–16. doi: 10.1111/j.1750-3639.2011.00504.x
 36. Mizuno K, Hida H, Masuda T, Nishino H, Togari H. Pretreatment with low doses of erythropoietin ameliorates brain damage in periventricular leukomalacia by targeting late oligodendrocyte progenitors: a rat model. *Neonatology* (2008) 94:255–66. doi: 10.1159/000151644
 37. Misumi S, Ueda Y, Nishigaki R, Suzuki M, Ishida A, Jung CG, et al. Dysfunction in motor coordination in neonatal white matter injury model without apparent neuron loss. *Cell Transplant.* (2016) 25:1381–93. doi: 10.3727/096368915X689893
 38. Ueda Y, Misumi S, Suzuki M, Ogawa S, Nishigaki R, Ishida A, et al. Disorganization of oligodendrocyte development in the layer II/III of the sensorimotor cortex causes motor coordination dysfunction in a model of white matter injury in neonatal rats. *Neurochem Res.* (2017) 43:127–37. doi: 10.1007/s11064-017-2352-3
 39. Ramanathan D, Conner JM, Tuszynski MH. A form of motor cortical plasticity that correlates with recovery of function after brain injury. *Proc Natl Acad Sci USA.* (2006) 103:11370–5. doi: 10.1073/pnas.0601065103
 40. Girgis J, Merrett D, Kirkland S, Metz GA, Verge V, Fouad K. Reaching training in rats with spinal cord injury promotes plasticity and task specific recovery. *Brain* (2007) 130:2993–3003. doi: 10.1093/brain/awm245
 41. Krajacic A, Ghosh M, Puentes R, Pearse DD, Fouad K. Advantages of delaying the onset of rehabilitative reaching training in rats with incomplete spinal cord injury. *Eur J Neurosci.* (2009) 29:641–51. doi: 10.1111/j.1460-9568.2008.06600.x
 42. Ishida A, Isa K, Umeda T, Kobayashi K, Kobayashi K, Hida H, et al. Causal link between the cortico-rubral pathway and functional recovery through forced impaired limb use in rats with stroke. *J Neurosci.* (2016) 36:455–67. doi: 10.1523/JNEUROSCI.2399-15.2016
 43. Koyama Y, Nishida T, Tohyama M. Establishment of an optimised protocol for a Golgi-electron microscopy method based on a Golgi-Cox staining procedure with a commercial kit. *J Neurosci Methods* (2013) 218:103–9. doi: 10.1016/j.jneumeth.2013.05.004
 44. Ishida A, Misumi S, Ueda Y, Shimizu Y, Cha-Gyun J, Tamakoshi K, et al. Early constraint-induced movement therapy promotes functional recovery and neuronal plasticity in a subcortical hemorrhage model rat. *Behav Brain Res.* (2015) 284:158–66. doi: 10.1016/j.bbr.2015.02.022
 45. Paolicelli RC, Bolasco G, Pagani F, Maggi L, Scianni M, Panzanelli P, et al. Synaptic pruning by microglia is necessary for normal brain development. *Science* (2011) 333:1456–8. doi: 10.1126/science.1202529
 46. Miyamoto A, Wake H, Moorhouse AJ, Nabekura J. Microglia and synapse interactions: fine tuning neural circuits and candidate molecules. *Front Cell Neurosci.* (2013) 7:70. doi: 10.3389/fncel.2013.00070
 47. Kaur C, Rathnasamy G, Ling EA. Biology of microglia in the developing brain. *J Neuropathol Exp Neurol.* (2017) 76:736–53. doi: 10.1093/jnen/nlx056
 48. Vilalta A, Brown GC. Neurophagy, the phagocytosis of live neurons and synapses by glia, contributes to brain development and disease. *FEBS J.* (2017). doi: 10.1111/febs.14323. [Epub ahead of print].
 49. Young NA, Vuong J, Teskey GC. Development of motor maps in rats and their modulation by experience. *J Neurophysiol.* (2012) 108:1309–17. doi: 10.1152/jn.01045.2011
 50. Jacobs KM, Donoghue JP. Reshaping the cortical motor map by unmasking latent intracortical connections. *Science* (1991) 251:944–7.
 51. Hu F, Strittmatter SM. Regulating axon growth within the postnatal central nervous system. *Semin Perinatol.* (2004) 28:371–8. doi: 10.1053/j.semperi.2004.10.001
 52. Wake H, Moorhouse AJ, Jinno S, Kohsaka S, Nabekura J. Resting microglia directly monitor the functional state of synapses *in vivo* and determine the fate of ischemic terminals. *J Neurosci.* (2009) 29:3974–80. doi: 10.1523/JNEUROSCI.4363-08.2009
 53. Kettenmann H, Kirchhoff F, Verkhratsky A. Microglia: new roles for the synaptic stripper. *Neuron* (2013) 77:10–18. doi: 10.1016/j.neuron.2012.12.023
 54. Miyamoto A, Wake H, Ishikawa AW, Eto K, Shibata K, Murakoshi H, et al. Microglia contact induces synapse formation in developing somatosensory cortex. *Nat Commun.* (2016) 7:12540. doi: 10.1038/ncomms12540
 55. Johnston MV, Hagberg H. Sex and the pathogenesis of cerebral palsy. *Dev Med Child Neurol.* (2007) 49:74–8. doi: 10.1017/S0012162207000199.x
 56. Constable RT, Ment LR, Vohr BR, Kesler SR, Fulbright RK, Lacadie C, et al. Prematurely born children demonstrate white matter microstructural differences at 12 years of age, relative to term control subjects: an investigation of group and gender effects. *Pediatrics* (2008) 121:306–16. doi: 10.1542/peds.2007-0414
 57. Sanches EF, Arteni NS, Nicola F, Boisserand L, Willborn S, Netto CA. Early hypoxia-ischemia causes hemisphere and sex-dependent cognitive impairment and histological damage. *Neuroscience* (2013) 237:208–15. doi: 10.1016/j.neuroscience.2013.01.066
 58. Sanches EF, Arteni NS, Scherer EB, Kolling J, Nicola F, Willborn S, et al. Are the consequences of neonatal hypoxia-ischemia dependent on animals' sex and brain lateralization? *Brain Res.* (2013) 1507:105–14. doi: 10.1016/j.brainres.2013.02.040
 59. Ayoub AE, Salm AK. Increased morphological diversity of microglia in the activated hypothalamic supraoptic nucleus. *J Neurosci.* (2003) 23:7759–66. doi: 10.1523/JNEUROSCI.23-21-07759.2003
 60. Perkins AE, Piazza MK, Deak T. Stereological analysis of microglia in aged male and female fischer 344 rats in socially relevant brain regions. *Neuroscience* (2018) 377:40–52. doi: 10.1016/j.neuroscience.2018.02.028

Conflict of Interest Statement: The authors declare that the research was conducted in the absence of any commercial or financial relationships that could be construed as a potential conflict of interest.

Copyright © 2018 Ueda, Bando, Misumi, Ogawa, Ishida, Jung, Shimizu and Hida. This is an open-access article distributed under the terms of the Creative Commons Attribution License (CC BY). The use, distribution or reproduction in other forums is permitted, provided the original author(s) and the copyright owner are credited and that the original publication in this journal is cited, in accordance with accepted academic practice. No use, distribution or reproduction is permitted which does not comply with these terms.